

Climate Hazard Assessment for Stakeholder Adaptation Planning in New York City

RADLEY M. HORTON

Center for Climate Systems Research, Earth Institute, Columbia University, and NASA Goddard Institute for Space Studies, New York, New York

VIVIEN GORNITZ AND DANIEL A. BADER

Center for Climate Systems Research, Earth Institute, Columbia University, New York, New York

ALEX C. RUANE

NASA Goddard Institute for Space Studies, and Center for Climate Systems Research, Earth Institute, Columbia University, New York, New York

RICHARD GOLDBERG

Center for Climate Systems Research, Earth Institute, Columbia University, New York, New York

CYNTHIA ROSENZWEIG

NASA Goddard Institute for Space Studies, and Center for Climate Systems Research, Earth Institute, Columbia University, New York, New York

(Manuscript received 25 March 2010, in final form 23 May 2011)

ABSTRACT

This paper describes a time-sensitive approach to climate change projections that was developed as part of New York City's climate change adaptation process and that has provided decision support to stakeholders from 40 agencies, regional planning associations, and private companies. The approach optimizes production of projections given constraints faced by decision makers as they incorporate climate change into long-term planning and policy. New York City stakeholders, who are well versed in risk management, helped to preselect the climate variables most likely to impact urban infrastructure and requested a projection range rather than a single "most likely" outcome. The climate projections approach is transferable to other regions and is consistent with broader efforts to provide climate services, including impact, vulnerability, and adaptation information. The approach uses 16 GCMs and three emissions scenarios to calculate monthly change factors based on 30-yr average future time slices relative to a 30-yr model baseline. Projecting these model mean changes onto observed station data for New York City yields dramatic changes in the frequency of extreme events such as coastal flooding and dangerous heat events. On the basis of these methods, the current 1-in-10-year coastal flood is projected to occur more than once every 3 years by the end of the century and heat events are projected to approximately triple in frequency. These frequency changes are of sufficient magnitude to merit consideration in long-term adaptation planning, even though the precise changes in extreme-event frequency are highly uncertain.

1. Introduction

This paper describes a methodological approach to stakeholder-driven climate hazard assessment developed for the New York, New York, metropolitan region (Fig. 1).

Corresponding author address: Radley Horton, Columbia University Center for Climate Systems Research, 2880 Broadway, New York, NY 10025.
E-mail: rh142@columbia.edu

The methods were developed in support of the New York City Panel on Climate Change (NPCC; Rosenzweig and Solecki 2010). The NPCC is an advisory body to New York City's Climate Change Adaptation Task Force (CCATF), formed by Mayor Michael Bloomberg in 2008 and overseen by the Mayor's Office of Long Term Planning and Sustainability. As described in Rosenzweig and Solecki (2010), the CCATF is composed of stakeholders from 40 city and state agencies, authorities, regional

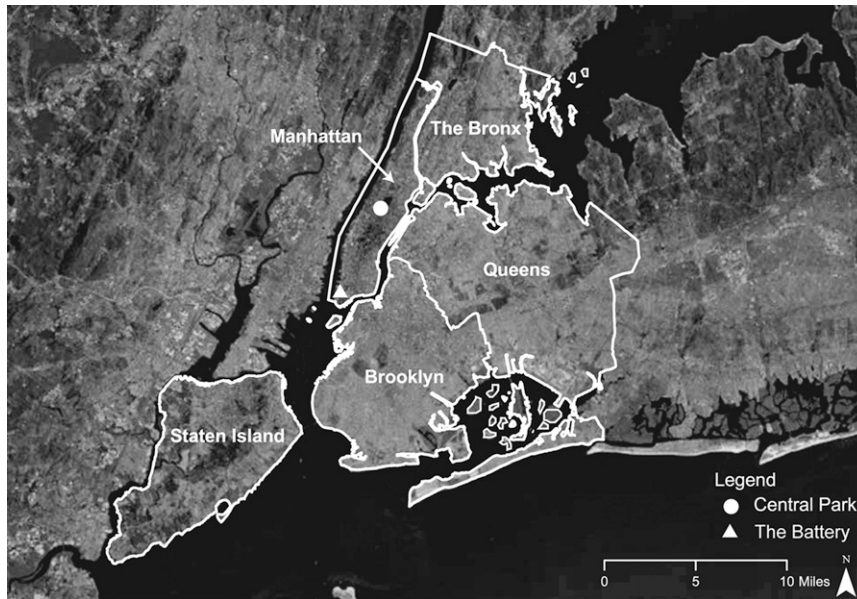


FIG. 1. Satellite map of the New York metropolitan region. Shown on the map are the Central Park weather station (circle) and the Battery tide gauge (triangle). Source: Esri World Imagery.

planning associations, and private companies, divided into four infrastructure working groups (communication, energy, transportation, and water and waste) and one policy working group.

The CCATF effort was motivated by the fact that the population and critical infrastructure of New York City (NYC) are exposed to a range of climate hazards, with coastal flooding associated with storms and sea level rise the most obvious threat. Approximately 7% (11%) of the NYC area is within 1 m (2 m) of sea level (Weiss et al. 2011). A recent study ranked NYC seventh globally among port cities in exposed population and second globally in assets exposed to storm-surge flooding and high winds (Nicholls et al. 2008). Furthermore, because NYC, like much of the United States (ASCE 2009), has aging infrastructure, climate vulnerability may be enhanced. By showing leadership in the infrastructure adaptation process, the NYC effort may be able to provide lessons to other cities as they plan adaptation strategies.

Stakeholder input regarding climate information was collected in several ways. Between September of 2008 and September of 2009, each CCATF sector working group held monthly meetings in conjunction with the Mayor's Office of Long Term Planning and Sustainability. During the initial meetings, representatives from each sector identified key climate hazards; they also interacted iteratively with the scientists, seeking clarification and requesting additional information. They commented on draft documents that describe the region's climate hazards, and climate seminars were held with individual agencies as requested. The climate hazard

assessment process was facilitated by prior collaborative experience between the NPCC's climate scientists and stakeholders in earlier assessments, including the Metro East Coast Study (Rosenzweig and Solecki 2001), as well as work with the New York City Department of Environmental Protection (NYCDEP; NYCDEP 2008; Rosenzweig et al. 2007) and the Metropolitan Transportation Authority (MTA; MTA 2007).

The climate hazard approach is tailored toward impact assessment; it takes into consideration the resource and time constraints faced by decision makers as they incorporate climate change into their long-term planning. For example, the formal write-up of the climate risk information was needed within less than 8 months of the NPCC's launch (National Research Council 2009); given this time frame and the broad array of stakeholders in the CCATF, a standardized set of climate variables of broad interest was emphasized, with the understanding that future studies could provide climate information tailored to unique applications.¹

Within this framework, the NPCC worked with stakeholders to preselect for analysis those climate variables and metrics that are most likely to impact existing

¹ For example, a tailored assessment of changes in snow depth and timing of snowmelt in the Catskill Mountains approximately 100 mi (160 km) north of NYC (NYCDEP 2008) would be of interest to managers of only a small but important subset of infrastructure—reservoirs and water tunnels. Such a finescale assessment would benefit from more complex downscaling approaches than those applied here.

assets, planned investments, and operations (Horton and Rosenzweig 2010). For example, the number of days below freezing was identified as an important metric for many sectors because of the impacts of freeze–thaw cycles on critical infrastructure (this process took place over 2008–09 at CCATF and working group meetings of the Mayor’s Office of Long Term Planning and Sustainability). Because of the diversity of agencies, projections were requested for multiple time periods spanning the entire twenty-first century.

Stakeholders also helped to determine the presentation of climate hazard information. Because NYC stakeholders are used to making long-term decisions under uncertainty associated with projections of future revenues, expenditures, and population trends, for example, they (CCATF) preferred projection ranges to a single “most likely” value.

Itemized risks associated with each climate variable were ultimately mapped to specific adaptation strategies. For example, more frequent and intense coastal flooding due to higher mean sea level was linked to increased seawater flow into New York City’s gravity-fed and low-lying wastewater pollution control plants, resulting in reduced ability to discharge treated effluent (Rosenzweig and Solecki 2010; NYCDEP 2008). NYCDEP is reducing the risk at the Far Rockaway Wastewater Treatment Plant by raising pumps and electrical equipment to 14 ft (4.3 m) above sea level on the basis of the projections described here (New York City Office of the Mayor 2009).

Climate hazard assessment was only one component of the NPCC’s impact and adaptation assessment. Vulnerability of infrastructure (and the populations that rely on it) to climate impacts can be driven as much by its state of repair (and how it is used) as by climate hazards (National Research Council 2009). Climate adaptation strategies should be based on many nonclimate-related factors, such as cobenefits (e.g., some infrastructure investments that reduce climate risks will also yield more efficient and resilient infrastructure in the face of nonclimate hazards; National Research Council 2010a) and cocosts (e.g., adapting by using more air conditioning increases greenhouse gas emissions). NPCC experts in the risk management, insurance, and legal fields provided guidance on these broader issues of vulnerability and adaptation, developing, for example, an eight-step adaptation assessment process and templates for ranking relative risk and prioritizing adaptation strategies (Rosenzweig and Solecki 2010). This paper focuses on the provision of stakeholder-relevant climate information in support of the broader NPCC assessment.

Section 2 describes the method used for the NPCC’s climate hazard assessment. Section 3 compares climate-model hindcasts with observational results for the New

York metropolitan region. Hindcast results are a recurring stakeholder request, and they helped to inform the global climate model (GCM)–based projection methods. Section 4 documents the regional projections in the context of stakeholder usability. Section 5 covers conclusions and recommendations for future work.

2. Methods

a. Observations

Observed data are from two sources. Central Park station data from the National Oceanic and Atmospheric Administration National Climatic Data Center U.S. Historical Climatology Network, version 1, dataset (Karl et al. 1990; Easterling et al. 1999; Williams et al. 2005) formed the basis of the historical analysis and projections of temperature and precipitation. Gridded output corresponding to NYC from the National Centers for Environmental Prediction–U.S. Department of Energy (NCEP–DOE) Reanalysis 2 dataset (Kanamitsu et al. 2002) is also used for GCM temperature validation (section 3).

b. Climate projections: General approach

1) GLOBAL CLIMATE MODELS AND EMISSIONS SCENARIOS

Climate projections are based on the coupled GCMs used for the Intergovernmental Panel on Climate Change Fourth Assessment Report (IPCC AR4; Solomon et al. 2007). The outputs are provided by the World Climate Research Programme (WCRP) Coupled Model Intercomparison Project, phase 3, (CMIP3) multimodel dataset (Meehl et al. 2007a). Of 23 available GCM configurations from 16 centers, selected were the 16 GCMs that had available output for all three emissions scenarios (“A2,” “A1B,” and “B1”) from the IPCC Special Report on Emissions Scenarios (SRES; Nakicenovic et al. 2000) and that were archived by the WCRP (Table 1).

The 16 GCMs and three emissions scenarios combine to produce 48 output sets. The 48 members yield a model- and scenario-based distribution function that is based on equal weighting of each GCM and emissions scenario. The model-based results should not be mistaken for a statistical probability distribution (Brekke et al. 2008) for reasons including the following: 1) no probabilities are assigned by the IPCC to the emissions scenarios²; 2) GCMs are not completely independent,

² It has been argued that, because high growth rates of global anthropogenic carbon dioxide emissions (3.4% yr⁻¹ between 2000 and 2008; Le Quere et al. 2009) led to 2008 estimated emissions reaching the levels of the highest SRES scenario (“A1FI”), other SRES scenarios may be unrealistically low.

TABLE 1. Acronym, host center, atmosphere and ocean gridbox resolution, and reference for the 16 GCMs used in the analysis.

Model acronym	Institution	Atmospheric resolution (lat × lon)	Oceanic resolution (lat × lon)	References
BCCR-BCM	Bjerknes Center for Climate Research (Norway)	1.9 × 1.9	0.5–1.5 × 1.5	Furevik et al. (2003)
CCSM	National Center for Atmospheric Research	1.4 × 1.4	0.3–1.0 × 1.0	Collins et al. (2006)
CCCMA-CGCM	Canadian Centre for Climate Modeling and Analysis	2.8 × 2.8	1.9 × 1.9	Flato (2010)
CNRM	National Weather Research Center, Météo-France	2.8 × 2.8	0.5–2.0 × 2.0	Terray et al. (1998)
CSIRO_Mk3	CSIRO Atmospheric Research (Australia)	1.9 × 1.9	0.8 × 1.9	Gordon et al. (2002)
MPI-ECHAM5	Max Planck Institute for Meteorology	1.9 × 1.9	1.5 × 1.5	Jungclaus et al. (2006)
MIUB-ECHO-G	Meteorological Institute of the University of Bonn	3.75 × 3.75	0.5–2.8 × 2.8	Min et al. (2005)
GFDL-CM2.0	Geophysical Fluid Dynamics Laboratory	2.0 × 2.5	0.3–1.0 × 1.0	Delworth et al. (2006)
GFDL-CM2.1	Geophysical Fluid Dynamics Laboratory	2.0 × 2.5	0.3–1.0 × 1.0	Delworth et al. (2006)
GISS	NASA Goddard Institute for Space Studies	4.0 × 5.0	4.0 × 5.0	Schmidt et al. (2006)
INMCM	Institute for Numerical Mathematics (Russia)	4.0 × 5.0	2.0 × 2.5	Volodin and Diansky (2004)
IPSL	Pierre Simon Laplace Institute (France)	2.5 × 3.75	2.0 × 2.0	Marti et al. (2005)
MIROC	Frontier Research Center for Global Change (Japan)	2.8 × 2.8	0.5–1.4 × 1.4	K-1 Model Developers (2004)
MRI-CGCM	Meteorological Research Institute (Japan)	2.8 × 2.8	0.5–2.0 × 2.5	Yukimoto and Noda (2003)
PCM	National Center for Atmospheric Research	2.8 × 2.8	0.5–0.7 × 1.1	Washington et al. (2000)
UKMO-HadCM3	Hadley Center for Climate Prediction, Met Office	2.5 × 3.75	1.25 × 1.25	Johns et al. (2006)

with many sharing portions of their code and a couple differing principally in resolution only; and 3) the GCMs and emissions scenarios do not sample all possible outcomes, which include the possibility of large positive ice-albedo and carbon-cycle feedbacks, in addition to uncertain aerosol effects. Caveats notwithstanding, the model-based approach has the advantage (relative to projections based on single numbers) of providing stakeholders with a range of possible outcomes associated with uncertainties in future greenhouse gas concentrations, other radiatively important agents, and climate sensitivity (National Research Council 2010b).

Some authors (e.g., Smith et al. 2009; Tebaldi et al. 2005; Greene et al. 2006; Brekke et al. 2008; Giorgi and Mearns 2002) have explored alternate approaches that weight GCMs on the basis of criteria that include hindcasts of regional climate or key physical processes. There are several reasons why that more complex approach is eschewed here in favor of equal GCM weighting. First, because model “success” is often region specific and variable specific and because stakeholders differ in their climate variables and geographical ranges of interest,³ production of consistent scenarios that are based on model weighting is a major research effort beyond the scope of NYC’s initial assessment. Second, although long-term research could be geared toward developing optimized multivariate (and/or multiregion) weighting, research suggests that compensating biases tend to yield comparable model performance (Brekke et al. 2008). Third,

historical accuracy may have been achieved for the “wrong” reasons (Brekke et al. 2008) and GCM hindcasts did not share identical forcing, especially with respect to aerosols (Rind et al. 2009). Fourth, shifting climate processes with climate change may favor different models in the future. Fifth, the elimination of ensemble members reduces the representation of uncertainty relating to climate sensitivity.

2) TIME SLICES

Because current-generation GCMs used for climate change applications have freely evolving ocean and atmospheric states, they are most appropriate for detection of long-term climate and climate change signals. The 30-yr time slice applied here is a standard time scale (World Meteorological Organization 1989) that represents a middle ground, allowing partial cancellation of currently unpredictable interannual-to-interdecadal variability (achieved by including many years) while maintaining relatively monotonic anthropogenically induced forcing trends (achieved by including few years). The “1980s” time slice represents baseline conditions between 1970 and 1999; future time slices for the 2020s, 2050s, and 2080s are similarly defined.

3) CLIMATE CHANGE FACTORS AND THE DELTA METHOD

Mean temperature change projections are expressed as differences between each model’s future time-slice simulation and its baseline simulation; mean precipitation is based on the ratio of a given model’s future to its baseline values. This approach offsets a large source of model bias: poor GCM simulation of local baseline

³ NYC’s task force included corporations with national and international operations.

conditions (section 3b) arising from a range of factors, including the large difference in spatial resolution between GCM grid boxes and station data.

Because monthly averages from GCMs are generally more reliable than daily output (Grotch and MacCracken 1991), monthly mean GCM changes were projected onto observed 1971–2000 daily Central Park data for the calculation of extreme events.⁴ This simple and low-cost downscaling approach is known as the delta method (Gleck 1986; Arnell 1996; Wilby et al. 2004). Like more complex statistical downscaling techniques (e.g., Wigley et al. 1990), the delta method is based on stationarity (e.g., Wilby et al. 1998, 2002; Wood et al. 2004) and largely excludes the possibility of large variance changes through time, although for the northeastern United States such changes are uncertain.⁵

More complex statistical approaches, such as those that empirically link large-scale predictors from a GCM to local predictands (e.g., Bardossy and Plate 1992) may yield more nuanced downscaled projections than does the delta method. These projections are not necessarily more realistic, however. Historical relationships between large-scale predictors and more impacts-relevant local predictands may not be valid in a changing climate (Wilby et al. 2004). GCM development and evaluation have also historically been more focused on seasonal and annual climatological distributions than on the daily and inter-annual distributions that drive analog approaches. Table 2 provides a set of stakeholder questions to inform the choice of downscaling technique—a topic that is discussed further in section 5.

4) SPATIAL EXTENT

The projections are for the land-based GCM grid box covering NYC. As shown in Fig. 2, the 30-yr averaged mean climate changes are largely invariant at subregional scales; the single gridbox approach produces results that are nearly identical to those of the more complex methods that require extraction of data from multiple grid boxes and weighted spatial interpolation. As shown in section 4d, for the metrics evaluated in this study, the GCM gridbox results also produce results that are comparable to those of finer-resolution statistically and dynamically downscaled products. Because baseline climate (as opposed to projected climate change) does differ

dramatically over small spatial scales (because of factors such as elevation and surface characteristics), and because these finescale spatial variations by definition cannot be captured by coarse-resolution GCMs, GCM changes are trained onto observed Central Park data using the procedures described in section 2b(3).

5) NUMBER OF SIMULATIONS

For 13 of the 16 GCMs' climate of the twentieth century and future A1B experiments, and for the climates of 7 of the 16 B1 and A2 future experiments, multiple simulations driven by different initial conditions were available. Analysis of hindcasts and projections (Table 3) from the available National Center for Atmospheric Research (NCAR) Community Climate System Model (CCSM) coupled GCM simulations⁶ revealed only minor variations in 30-yr averages, suggesting that one simulation per model is sufficient. Using an ensemble for each GCM that is based on all of the available simulations with that GCM is an alternative approach; the effort and data storage needs may not be justified, however, given the similarity of the ensemble and individual simulation results shown in Table 3. Furthermore, ensemble averaging unrealistically shrinks the temporal standard deviation.⁷

c. Climate projections: Sea level rise

To address large uncertainties associated with future melting of ice sheets, two projection methods for sea level rise were developed. These methods are referred to as the IPCC-based and rapid ice melt scenarios, respectively.

1) IPCC AR4-BASED APPROACH

The IPCC AR4 approach (Meehl et al. 2007b) was regionalized for NYC, utilizing four factors that contribute to sea level rise: global thermal expansion, local water surface elevation, local land uplift/subsidence, and global meltwater.⁸ Thermal expansion and local water surface elevation terms are derived from the GCMs (outputs were provided through the courtesy of WCRP and Dr. J. Gregory 2007, personal communication). Local land subsidence is derived from Peltier (2001) and Peltier's "ICE-5G," version 1.2, ice model (from 2007) (obtained online at <http://www.pol.ac.uk/psmsl/peltier/index.html>). The meltwater term was calculated using

⁴ For coastal flooding and drought, the twentieth century was used as a baseline because of high interannual/multidecadal variability and policy relevance of 1-in-100-yr events.

⁵ An exception may be short-term precipitation variance, which is expected to increase regionally with the more intense precipitation events associated with a moister atmosphere (e.g., Emori and Brown 2005; Cubasch et al. 2001; Meehl et al. 2005).

⁶ This GCM was selected because it provided the most twentieth- and twenty-first-century simulations.

⁷ This is a general criticism; for the particular case in which the delta method is used (as here), shrinking of the temporal standard deviation has no bearing on the results.

⁸ Only seven GCMs provided outputs for projections of sea level rise; see Horton and Rosenzweig (2010) for additional information.

TABLE 2. Checklist of questions to inform selection of climate hazard assessment and projection methods.

Question	Possible implication for choice of method, plus NYC context
1) Are high-quality historical data available for a long time period?	When few high-quality historical climate data are available, options for projections are extremely limited. Records of at least several decades are needed to sample the range of natural variability. As regional climate models (RCM) continue to improve, use of raw outputs from RCMs may increasingly be used in such regions, since bias correction and statistical approaches are not feasible without historical climate data. This was not an issue in data-rich NYC.
2) Are projections needed for the entire twenty-first century?	If yes, this may preclude RCMs because of computational expense. This was an important consideration for NYC, since some sectors such as telecommunications were focused on the 2020s time slice while others such as Port Authority of New York and New Jersey manage infrastructure that is expected to last until 2100.
3) Are multiple emissions scenarios needed—for example, to emphasize how mitigation can complement adaptation?	If yes, RCMs may not be the best approach, since computational expense generally precludes the use of more than one or two scenarios. This was an important consideration in NYC, since the adaptation effort was part of a broader sustainability effort (“PlaNYC”) that embraced greenhouse gas mitigation.
4) Are a large group of GCMs and initializations required, so as to sample a broad range of global climate sensitivities and estimates of within-GCM variability, respectively?	If yes, RCMs may not be the best approach, since computational expense generally precludes the use of more than a few GCMs or GCM initializations per RCM. NYC stakeholders expressed interest in the full range of GCM sensitivities.
5) What climate variables are needed, and are they available at the necessary spatial and temporal resolutions within public climate-model archives?	In NYC, relatively few variables were needed and subdaily information was not required. Additional variable needs at subdaily resolution might argue for the use of RCM archives such as NARCCAP as they continue to be populated, instead of archives such as the first generation of bias-corrected and spatially disaggregated data (BCSD) (monthly temperature and precipitation only). Although use of public climate-model archives minimizes cost and time, even archived outputs generally require at least some bias and/or scale correction and postprocessing for stakeholder applicability.
6) What level of resources are available, and in what time frame is the information needed?	Region- and question-specific tailored downscaling efforts, as opposed to use of archived downscaled products, may not be possible when resources and time are limited. NYC had substantial resources available, but the short time frame (~8 months) precluded developing new tailored downscaling.
7) Are projections needed for a single in-depth sectoral application and variable in one municipality, or does a large multisectoral and panregional group of stakeholders need a coordinated set of scenarios covering a series of standard variables?	In tailored statistical downscaling the method is optimized to the particular location and/or variable. When many variables and a larger region are included, no single optimization method will generally be best for all variables and locations, potentially leading to inconsistencies in either methods or projections across variables and locations. In NYC, the initial emphasis was on generating a common denominator of consistent scenarios based on consistent methods (the delta method) to facilitate coordination across 40 stakeholder entities.
8) Are high-frequency climate inputs that are continuous in time and space required, such as for input into an impacts model (e.g., a hydrological model to assess turbidity)?	If an impacts model is to be run with climate outputs, the range of climate and impact results (rather than just the “delta” mean) will likely be of interest, which may argue for a downscaling technique that allows variance to change, such as BCSD. Statistical downscaling techniques that include weather generators [such as the Statistical Downscaling Model (SDSM)] may be desirable to create a long record at the needed resolution that includes a range of extreme outcomes for planning purposes. The larger the continuous geographic domain (e.g., a large watershed) is, the greater is the need for caution regarding weather-generator treatment of spatiotemporal correlation. Although impacts modeling was not the initial thrust of the NYC CCATF effort, climate scenarios for impact modeling are being developed for specific sectors (e.g., NYCDEP 2008).
9) Is the region’s climate characterized by large spatial heterogeneity?	If not, applying the delta method to a single GCM grid box may be justifiable for many applications, as it was in NYC.
10) Are modes of variability important and predictable?	If not, the use of 30-yr time slices (and the delta method) that emphasize the signal of greenhouse gases and other radiatively important agents should be emphasized, as was done for NYC.

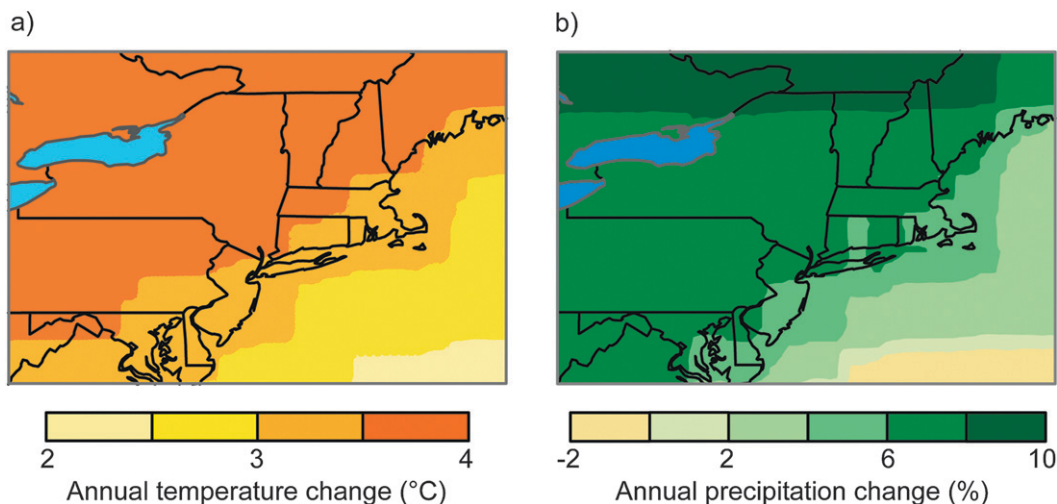


FIG. 2. (a) Temperature change ($^{\circ}\text{C}$) and (b) precipitation change (%) for the 2080s time slice relative to the 1970–99 model baseline, A1B emissions scenario, and 16-GCM ensemble mean.

mass-balance temperature-sensitivity coefficients for the different ice masses on the basis of observed historic relationships among global mean surface air temperature, ice mass, and rates of sea level rise (Meehl et al. 2007b).⁹ Regionalization of projections of sea level rise, on the basis of the four components described above, has been used in other studies (e.g., Mote et al. 2008).

2) RAPID ICE MELT SCENARIO

Because of large uncertainties in dynamical ice sheet melting (Hansen et al. 2007; Horton et al. 2008) and recent observations that ice sheet melting has accelerated within this past decade (e.g., Chen et al. 2009), an alternative sea level rise scenario was developed. This upper-bound scenario of sea level rise allowing for rapid ice melt was developed on the basis of paleo-sea level analogs, in particular the $\sim 10\,000$ – $12\,000$ -yr period of rapid sea level rise following the end of the last ice age (Peltier and Fairbanks 2006; Fairbanks 1989). Although the analog approach has limitations (most notably, the continental ice supply is much smaller today; Rohling et al. 2008), past rapid rise is described below because it may help to inform discussions of upper bounds of future sea level rise.

Average sea level rise during this more-than-10 000-yr period after the last ice age was 9.9 – 11.9 $\text{cm} (10 \text{ yr})^{-1}$, although this rise was punctuated by several shorter episodes of more rapid sea level rise. In the rapid ice melt

scenario, glaciers and ice sheets are assumed to melt at that average rate. The meltwater term is applied as a second-order polynomial, with the average present-day ice melt rate of $1.1 \text{ cm} (10 \text{ yr})^{-1}$ for 2000–04 used as a base. This represents the sum of observed mountain-glacier (Bindoff et al. 2007) and ice-sheet melt (Shepherd and Wingham 2007) during this period. The rapid ice melt scenario replaces the IPCC meltwater term with the modified meltwater term; the other three sea level terms remain unchanged. This approach does not consider how rapid ice melt might indirectly influence sea level in the New York region through future second-order effects, including gravitational, glacial isostatic adjustment, and rotational terms (e.g., Mitrovica et al. 2001, 2009).

d. Climate projections: Extreme events

On the basis of stakeholder feedback, quantitative and qualitative projections were made using the extreme-events definitions that stakeholders currently use. For example, temperature extremes were defined on the basis of specific thresholds, such as 90°F ($\sim 32^{\circ}\text{C}$), that the NYC Department of Buildings uses to define cooling requirements, whereas coastal flooding was defined by frequency of occurrence (Solecki et al. 2010).

1) QUANTITATIVE PROJECTIONS: COASTAL FLOOD EXAMPLE

The coastal flooding projections are based on changes in mean sea level, not storms. Projected changes in mean sea level (using the IPCC AR4-based approach) were superimposed onto historical data. For coastal flooding, critical thresholds for decision making are the 1-in-10-yr

⁹ Corrections were not made to account for reductions in glacier area over time.

TABLE 3. NCAR CCSM mean climatological values of available simulations and CCSM ensemble for the grid box covering NYC for the 1970–99 hindcast and for the A1B 2080s (2070–99 average) relative to the same-simulation 1970–99 hindcast.

	1970–99 mean temperature (°C)	1970–99 mean precipitation (cm)	2080s A1B temperature change (°C)	2080s A1B precipitation change (%)
CCSM run1	9.38	98.03	3.44	2.81
CCSM run 2	9.27	91.88	3.32	10.15
CCSM run 3	9.67	92.08	3.03	12.44
CCSM run 5	9.42	94.87	3.24	9.75
CCSM run 6	9.64	95.22	2.75	9.56
CCSM run 7	9.64	91.30	2.96	12.03
CCSM run 9	9.68	94.69	3.01	10.36
CCSM ensemble	9.53	94.10	3.11	9.52

and 1-in-100-yr flood events (Solecki et al. 2010). The latter metric is a determinant of construction and environmental permitting, as well as flood insurance eligibility (Sussman and Major 2010).

The 1-in-10-yr event was defined by using historical hourly tide data from the Battery tide gauge in lower Manhattan [http://tidesandcurrents.noaa.gov; for more information, see Horton and Rosenzweig (2010)]. The 1-in-100-yr flood was analyzed using flood-return-period curves that are based on data provided by the U.S. Army Corps of Engineers for the Metro East Coast Regional Assessment [see Gornitz (2001) for details].

Because interannual variability is particularly large for rare events such as the 1-in-10-yr flood, a base period of more than the standard 30 years was used. Similarly, because each year between 1962 and 1965 was drier in Central Park than the driest year between 1971 and 2000, the entire twentieth-century precipitation record was used for the drought analysis. More-rigorous solutions for the rarest events await better predictions of interannual-to-multidecadal variability, better understanding of the relationship between variability at those time scales and extreme events (e.g., Namias 1966; Bradbury et al. 2002), and the growing event pool of realizations with time.

2) QUALITATIVE EXTREME-EVENT PROJECTIONS

The question arose of how best to meet stakeholder needs when scientific understanding, data availability, and model output are incomplete; quantitative projections are unavailable for some of the important climate hazards consistently identified by infrastructure stakeholders and/or are characterized by such large uncertainties as to render quantitative projections inadvisable. Examples in the NYC region include ice storms, snowfall, lightning, intense subdaily precipitation events, tropical storms, and northeasters. For these events, qualitative information was provided, describing only the most likely direction of change and an associated likelihood using the IPCC

Working Group I likelihood categories (Solomon et al. 2007).¹⁰ Sources of uncertainty and key historical events were also described to provide stakeholders with context and the opportunity to assess sectorwide impacts of historical extremes.

3. GCM hindcasts and observations

The results of the GCM hindcasts and observational analysis described in this section informed the development of the projection methods described in section 2. Stakeholders commonly request hindcasts and historical analysis (e.g., NYCDEP 2008) because they provide transparency to decision makers who may be new to using GCM projections as a planning tool.

a. Temperature and precipitation trends

As shown in Table 4, both the observed and modeled twentieth-century warming trends at the annual and seasonal scale are generally significant at the 99% level. Although GCM twentieth-century trends are generally approximately 50% smaller than the observed trends, it has been estimated that approximately one-third of NYC's twentieth-century warming trend may be due to urban heat island effects (Gaffin et al. 2008) that are external to GCMs. Over the 1970–99 period of stronger greenhouse gas forcing, the observed annual trend was $0.21^{\circ}\text{C} (10 \text{ yr})^{-1}$ and the ensemble trend was $0.18^{\circ}\text{C} (10 \text{ yr})^{-1}$.

¹⁰ Given the large impact of these extreme events on infrastructure, stakeholders requested information about likelihood for comparative purposes (e.g., “Which is more likely to increase in frequency: Northeasters specifically or intense precipitation events generally?”). Assignment of likelihood to generalized categories for qualitative extremes (on the basis of published literature and expert judgment, including peer review) was possible because predictions are general (e.g., direction of change), as opposed to the quantitative model-based projections.

TABLE 4. Annual and seasonal temperature [$^{\circ}\text{C}$ (10 yr^{-1})] and precipitation [cm (10 yr^{-1})] trends for the twentieth century and 1970–99. Shown are observed Central Park station data, the 16 GCM ensemble, and four points on the GCM distribution (lowest, 17th percentile, 83rd percentile, and highest). Only 15 GCMs were available for the twentieth-century hindcast.

	Min	17%	83%	Max	Ensemble	Obs
Twentieth-century temperature						
Annual	-0.03	0.02	0.12	0.17	0.07*	0.15*
DJF	-0.04	0.02	0.16	0.19	0.08*	0.20*
MAM	-0.05	-0.02	0.12	0.25	0.06*	0.18*
JJA	-0.02	0.03	0.11	0.15	0.07*	0.12*
SON	0.00	0.03	0.15	0.18	0.09*	0.08
1970–99 temperature						
Annual	-0.11	0.10	0.28	0.39	0.18*	0.21
DJF	-0.47	-0.05	0.35	0.51	0.11	0.76
MAM	-0.36	-0.15	0.41	0.74	0.14	0.10
JJA	-0.01	0.13	0.29	0.44	0.20*	0.05
SON	-0.06	0.13	0.50	0.70	0.29*	-0.03
Twentieth-century precipitation						
Annual	-1.22	-0.22	0.66	0.76	0.16	1.60
DJF	-0.23	-0.18	0.27	0.78	0.05	0.27
MAM	-0.27	-0.13	0.28	0.39	0.10	0.90
JJA	-0.69	-0.39	0.22	0.35	-0.07	-0.09
SON	-0.25	-0.08	0.32	0.46	0.10	0.61
1970–99 precipitation						
Annual	-3.52	0.02	2.05	5.73	0.87	-1.77
DJF	-3.21	-0.19	1.48	2.94	0.48	-0.48
MAM	-2.33	-1.37	1.05	1.98	-0.08	1.55
JJA	-2.08	-1.33	1.19	1.75	-0.03	-1.51
SON	-1.72	-0.55	1.89	2.93	0.48	-1.72

* Trend is significant at the 99% level.

Modeled seasonal warming trends in the past three decades and both annual and seasonal precipitation trends over the entire century for NYC generally deviate strongly from observations, consistent with prior results for the Northeast (e.g., Hayhoe et al. 2007). Observed and modeled trends in temperature and precipitation at a particular location are highly dependent on internal variability and therefore are highly sensitive to the selection of years. For example, the 1970–99 observed Central Park annual precipitation trend of -1.77 cm (10 yr^{-1}) shifts to 0.56 cm (10 yr^{-1}) when the analysis is extended through 2007. This is especially true for the damaging extreme events¹¹ (Christensen et al. 2007) that are often of particular interest to infrastructure managers.

¹¹ Among twentieth-century Central Park trends in observed extremes, only trends in cold extremes have been robust. For the number of days per year with minimum temperatures below freezing, both the 100-yr trend of -2 days (10 yr^{-1}) and the 30-yr trend of -5.2 days (10 yr^{-1}) are significant at the 99% level. GCM hindcasts of extreme events were not conducted because of the small signal-to-noise ratio.

In coupled GCM experiments with a freely evolving climate system, anomalies associated with climate variability generally will not coincide with observations, leading to departures between observed and modeled trends (Randall et al. 2007).

For stakeholders trained in analyzing recent local observations, it is challenging but important to emphasize that 1) trends at continental and centennial time scales are often most appropriate for identifying the greenhouse gas signal and GCM performance, since (unpredictable) interannual-to-interdecadal variability is lower at those scales (Hegerl et al. 2007), and 2) during the twenty-first century, higher greenhouse gas concentrations are expected to increase the role of the climate change signal, relative to climate variability.

b. Temperature and precipitation climatological values

Comparison of station data with a GCM grid box is hindered by the spatial-scale discrepancy; NYC's low elevation, urban heat island (see, e.g., Rosenzweig et al. 2006), and land–sea contrasts are not captured by GCMs. As shown in Fig. 3a, the observed average annual temperature over the 1970–99 period for New York City exceeds the GCM ensemble value by 2.6°C and is higher than those of all but 2 of the 16 GCMs. When the GCMs are contrasted with the spatially comparable NCEP–DOE reanalysis grid box, the annual mean temperature bias is reduced to 1.1°C . The departure of the Central Park station data from the GCM ensemble is largest in July and is smallest in January, indicating that the annual temperature cycle at this location is damped in the GCMs (Fig. 3b).

Although Fig. 3c reveals that the GCM ensemble of average annual precipitation from 1970 to 1999 is 8% below observations for Central Park, the ensemble average lies well within the range of precipitation for NYC as a whole; GCM precipitation exceeds the LaGuardia Airport station by 9%. Most of the GCMs are able to capture the relatively even distribution of monthly precipitation throughout the year (Fig. 3d).

The above analysis reveals that mean climatological departures from observations over the hindcast period are large enough to necessitate bias correction, such as the delta method as part of the GCM projection approach, rather than direct use of model output.

c. Temperature and precipitation variance

1) INTERANNUAL

Of the 16 GCMs, 11 overestimate the 1970–99 interannual standard deviation of temperature relative to the station data and 10 overestimate it relative to the

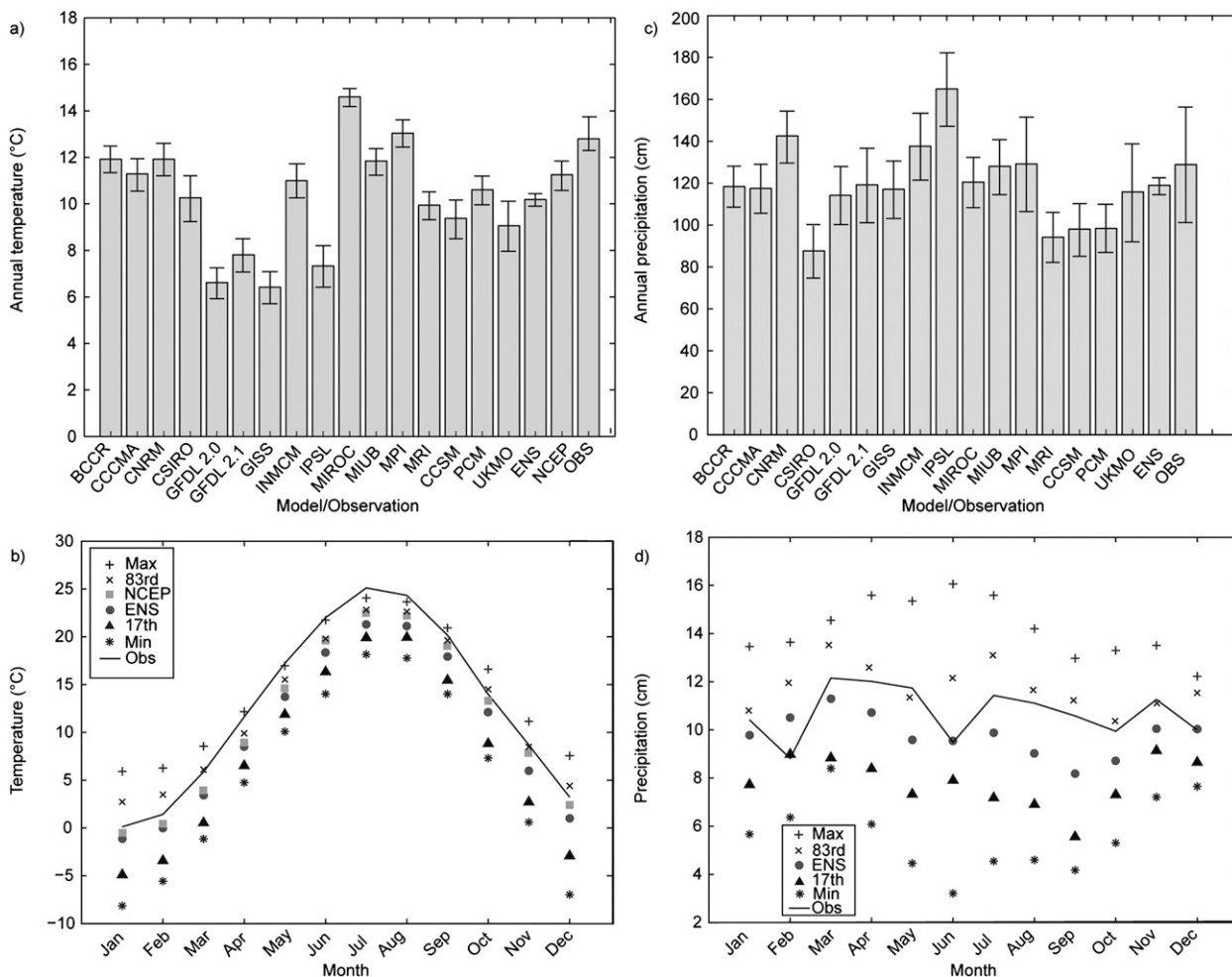


FIG. 3. (a) Mean annual temperature for the NYC region (°C), 1970–99, in each of the 16 GCMs, GCM ensemble, Central Park station data, and reanalysis (see section 2 for more information). Also shown as hash marks is the interannual standard deviation about the mean for each of the 19 products. (b) Monthly mean temperature for the NYC region (°C), 1970–99. The two observed products, the GCM ensemble average, and four points in the GCM distribution (lowest, 17th percentile, 83rd percentile, and highest) are shown. (c) Mean annual precipitation for the NYC region (cm), 1970–99, in each of the 16 GCMs, GCM ensemble, and Central Park observations. Also shown as hash marks is the interannual standard deviation about the mean for each of the 18 products. (d) Monthly mean precipitation for the NYC region (cm), 1970–99. Central Park observations, the GCM ensemble average, and four points in the GCM distribution (lowest, 17th percentile, 83rd percentile, and highest) are shown.

NCEP–DOE reanalysis. The similarities among GCMs, reanalysis, and station data suggest that spatial-scale discontinuities may not have a large impact on interannual temperature variance. All 16 GCMs underestimate interannual precipitation variability relative to Central Park observations, and 14 of the 16 GCMs underestimate variance relative to two other stations analyzed (Port Jervis and Bridgehampton). The large difference between the GCMs and station data suggests that spatial-scale discontinuities, likely associated with features like convective rainfall that cannot be resolved by GCMs, may be partially responsible for the relatively low modeled interannual precipitation variance. Observed

interannual temperature variance is greatest in winter—a pattern not captured by 7 of the 16 GCMs.

2) HIGH FREQUENCY

The daily distribution of observed Central Park temperature (Figs. 4a–c) and precipitation (Fig. 5) was compared with single gridbox output from 3 of the 16 GCMs used in the larger analysis. The three models were part of a subset with daily output stored in the WCRP/CMIP3 repository and were selected because (of the subset) they featured the highest resolution [coupled “ECHAM5”–Max Planck Institute for Meteorology Ocean Model (referred to here as MPI; Jungclaus et al. 2006)

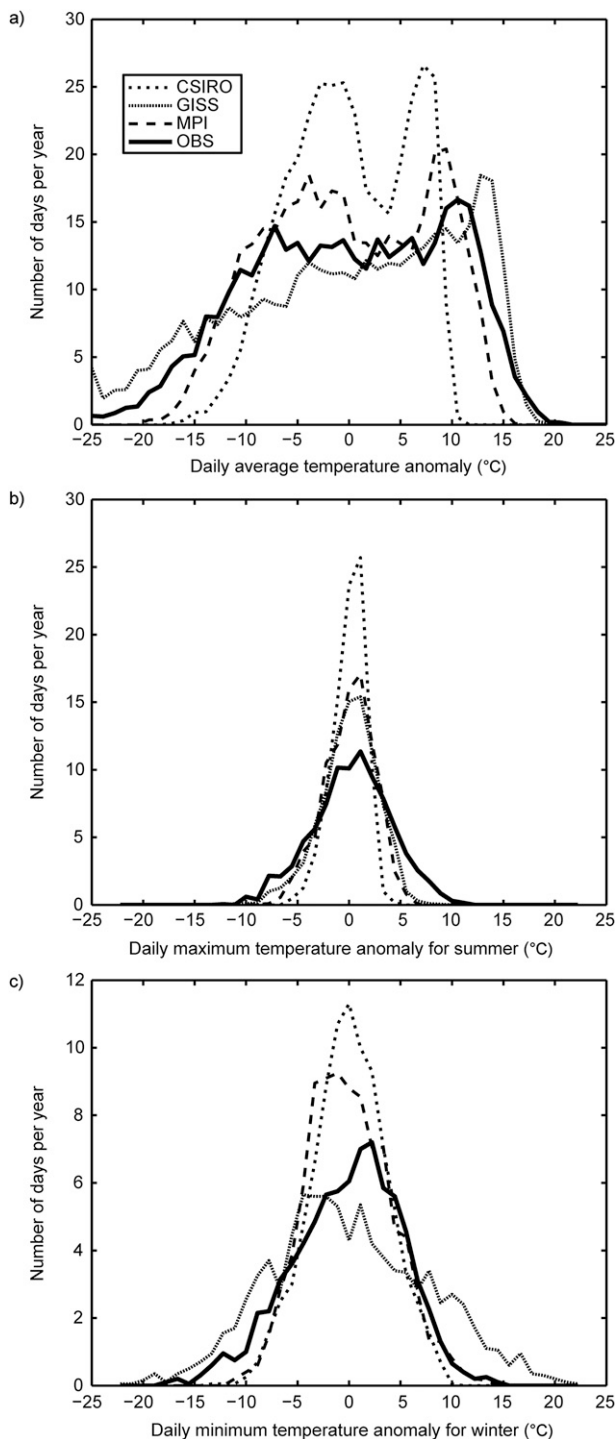


FIG. 4. Daily distribution (number of days per year) of (a) all-year mean, (b) summer (JJA) maximum, and (c) winter (DJF) minimum temperature anomalies ($^{\circ}\text{C}$) during 1980–99 for Central Park observations (solid line) and three GCMs (CSIRO, GISS, and MPI).

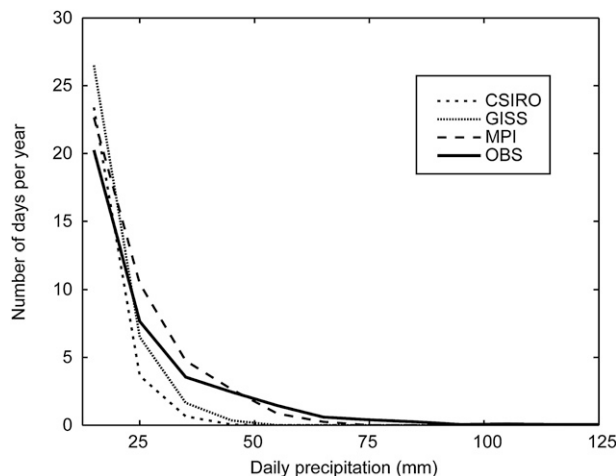


FIG. 5. Daily distribution (number of days per year) of precipitation (mm) during 1980–99 for Central Park observations (solid line) and three GCMs (CSIRO, GISS, and MPI). The first bin, containing less than 10 mm, is not shown.

and Commonwealth Scientific and Industrial Research Organisation, mark 3.0, model (CSIRO Mk3.0) (referred to here as CSIRO; Gordon et al. 2002), both at 1.88° latitude \times 1.88° longitude] and lowest resolution [National Aeronautics and Space Administration (NASA) Goddard Institute for Space Studies Model E-R (GISS-ER) (referred to here as GISS; Schmidt et al. 2006), at 4° latitude \times 5° longitude]. Analysis was conducted on summer [June–August (JJA)] daily maximum temperature and winter [December–February (DJF)] daily minimum temperature.

Summer maximum temperature distribution for the region in all three GCMs is narrower than that in the observations, and the warm tail is more poorly simulated than is the cold tail. During winter, CSIRO and MPI underestimate variance relative to the station data while the GISS GCM has excessive variance.

Figure 5 shows the number of days with precipitation exceeding 10 mm, which is a level of rainfall that can trigger combined sewer overflow events at vulnerable sites in NYC (PlaNYC 2008). Relative to Central Park data, all three GCMs underestimate the frequency of daily precipitation above 50 mm—a level of precipitation that can lead to widespread flooding and drainage problems, including in subways (MTA 2007).

Given that precipitation in GCMs of this class and spatial resolution is highly parameterized to the gridbox spatial scale and seasonal/decadal climate time scales, departures of the distribution from observed daily station data can be expected. The low model variance at daily time scales for temperature and precipitation, and at interannual time scales for precipitation, reinforces the need for statistical downscaling approaches such as

TABLE 5. Mean annual changes in temperature and precipitation for New York City, on the basis of 16 GCMs and three emissions scenarios. Shown is the central range (middle 67%) of values from model-based distributions; temperatures ranges are rounded to the nearest tenth of a degree, and precipitation is rounded to the nearest 5%.

	2020s	2050s	2080s
Air temperature	+0.8°–1.7°C	+1.7°–2.8°C	+2.2°–4.2°C
Precipitation	+0%–5%	+0%–10%	+5%–10%

the delta method that apply monthly mean model changes to observed high-frequency data.

d. Sea level rise

Sea level was also hindcast for the twentieth century, based on a 1990–99 projection relative to the 1900–04 base period.¹² The ensemble average hindcast is a rise of 18 cm, whereas the observed increase at the Battery is 25 cm. The 5-yr average local elevation term in the models meanders through time, frequently with an amplitude of 2–3 cm, with a maximum range over the century of approximately 7 cm, suggesting that decadal variability (primarily in the local elevation term) and spatial resolution may explain the discrepancy between models and observations.

4. Future projections

a. Mean temperature and precipitation

1) ANNUAL

Table 5 shows the projected changes in temperature and precipitation for the 30-yr periods centered around the 2020s, 2050s, and 2080s relative to the baseline period. The values shown are the central range (middle 67%) of the projected model-based changes.

Figure 6 expands upon the information presented in Table 5 in three ways. First, inclusion of observed data since 1900 provides context on how the scale of projected changes associated with forcing from greenhouse gases and other radiatively important agents compares to historical variations and trends. Second, tabulating high and low projections across all 48 simulations provides

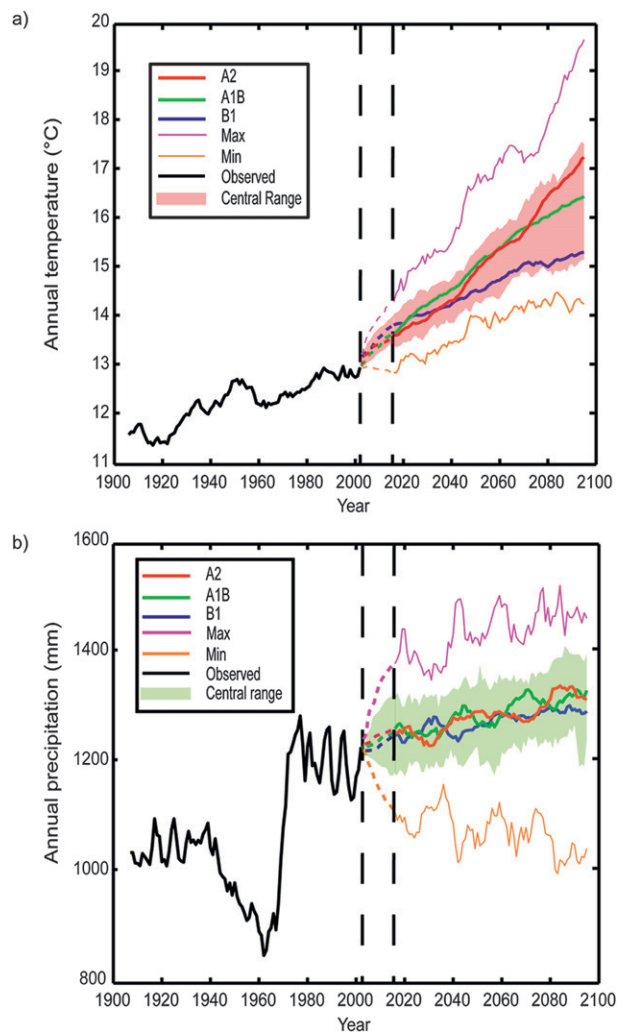


FIG. 6. Combined observed (black line) and projected (a) temperature (°C) and (b) annual precipitation (mm) for New York City. Projected model changes through time are applied to the observed historical data. The three thick lines (red, green, and blue) show the ensemble average for each emissions scenario across the 16 GCMs. Shading shows the central 67% range across the 16 GCMs and three emissions scenarios. The bottom and top lines, respectively, show each year's minimum and maximum projections across the suite of simulations. A 10-yr filter has been applied to the observed data and model output. The dotted area between 2003 and 2015 represents the period that is not covered because of the smoothing procedure.

a broader range of possible outcomes, which some stakeholders requested (New York City Climate Change Adaptation Task Force meetings over 2008–09). Third, ensemble averaging of results by emissions scenario as they evolve over time is informative to stakeholders involved in greenhouse gas mitigation (and adaptation), because it reveals the large system inertia: not until the 2030s and 2040s do the B1 scenario projections begin to diverge from A2 and A1B, but thereafter they diverge

¹² In this calculation, the land subsidence term was identical to that used for the twenty-first-century projections. The same surface mass-balance coefficients used by the IPCC, based on global average temperature changes over a 1961–2003 baseline, were used for the 1900–04 base period, which likely leads to a slight overestimate of the meltwater here. The effect is negligible, though, because the meltwater term is a minor contributor to the overall twentieth-century sea level rise.

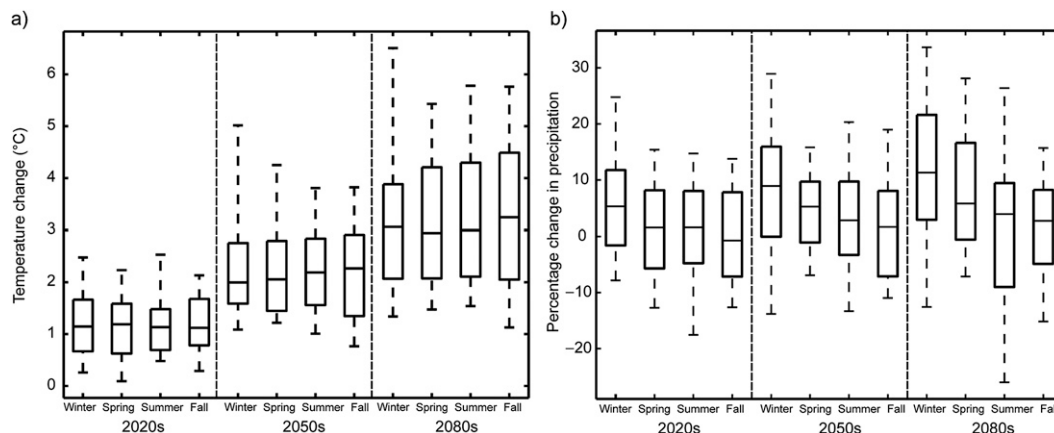


FIG. 7. Seasonal (a) temperature change ($^{\circ}\text{C}$) and (b) precipitation change (%) projections, relative to the 1970–99 model baseline, based on 16 GCMs and three emissions scenarios for the New York City metropolitan region. The maximum and minimum are shown as thin solid horizontal lines, the central 67% of values are boxed, and the median is the thick solid line inside the boxes.

rapidly. Thus, a delay in greenhouse gas mitigation activities greatly increases the risk of severe long-term climate change consequences, despite apparent similarity in the near-term outlook.

Although the precise numbers in Table 5 and Fig. 6 should not be emphasized because of high uncertainty and the smoothing effects of ensemble averaging, the stakeholder can see that in the New York metropolitan region 1) mean temperatures are projected to increase this century in all simulations, at rates exceeding those experienced in the twentieth century, 2) although precipitation is projected to increase slightly in most simulations, the multiyear precipitation range experienced in the past century as a result of climate variability exceeds the twenty-first-century climate change signal,¹³ and 3) climate projection uncertainties grow throughout the twenty-first century, in step with uncertainties regarding future emissions and the climate system response.

2) SEASONAL

Warming in the NYC region is of similar magnitude for all seasons in the GCMs, although seasonal projections are characterized by larger uncertainties than are annual

projections (Fig. 7a). The fact that interannual temperature variability is smallest in summer suggests that the summer warming may produce the largest departures from historical experience. Some impacts and vulnerabilities are also amplified by high temperatures. Energy demand in NYC is highly sensitive to temperature during heat waves, especially because of increased reliance on air conditioning. This increased demand can lead to elevated risk of power shortages and failures at a time when vulnerable populations are exposed to high heat stress and air pollution (Kinney et al. 2001; Hill and Goldberg 2001; Hogrefe et al. 2004).

GCMs tend to distribute much of the additional precipitation during the winter months (Fig. 7b), when water supply tends to be relatively high and demand tends to be relatively low (NYCDEP 2008). During September and October, a time of relatively high drought risk, total precipitation is projected by many models to decrease slightly.

b. Sea level rise

Addition of the two regional components leads to higher projections of sea level rise for the region than does the global average (by ~ 15 cm for end-of-century projections; Meehl et al. 2007b; Peltier 2001). This is due both to land subsidence and to higher sea level rise along the northeastern U.S. coast, the latter largely being due to geostrophic constraints associated with projected weakening of the Gulf Stream (Yin et al. 2009) in the results of many GCMs (Meehl et al. 2007b).

As shown in Table 6, the projections with the rapid ice melt scenario diverge from the IPCC-based approach as the century progresses. The 2100 value of up to ~ 2 m associated with this scenario (not shown) is generally

¹³ The projection lines in Fig. 6 depict the “predictable” anthropogenic forcing component while capturing some of the uncertainty associated with greenhouse gas concentrations and climate sensitivity at specific points in time. Because decadal variability is unpredictable in the Northeast, it was not included in the time-specific-projection portion of the figure. It was, however, emphasized to stakeholders that, while interannual variability appears to be greatly reduced in the projection portion of the figure, the observed portion (black line) reflects the kind of unpredictable variations that have been experienced in the past and that likely will exist on top of the mean change signal in the future.

TABLE 6. Sea level rise projections for New York City, on the basis of seven GCMs and three emissions scenarios. Shown is the central range (middle 67%) of values from model-based distributions rounded to the nearest centimeter. The scenario for rapid ice melt is based on recent rates of ice melt in the Greenland and West Antarctic Ice Sheets and on paleoclimatic studies. See the text for details.

	2020s	2050s	2080s
IPCC based	+5–13 cm	+18–30 cm	+30–54 cm
Rapid ice melt scenario	~13–25 cm	~48–74 cm	~104–140 cm

consistent with other recent results that roughly constrain sea level rise globally (e.g., Pfeffer et al. 2008; Rahmstorf 2007; Horton et al. 2008; Grinsted et al. 2009; Rignot and Cazenave 2009) and regionally (Yin et al. 2009; Hu et al. 2009) to between ~1 and ~2 m. The consistency with other studies supports the usefulness of ~2 m as a high end for a risk-averse approach to century-scale infrastructure investments, including bridges and tunnels, rail lines, and water infrastructure.

At the request of agencies that manage some of these long-term investments, two presentations were given to technical staff specifically describing the rapid ice melt method and projections. Although these and other stakeholders wanted to know the probability of the rapid ice melt scenario relative to the IPCC-based method, it was emphasized that such probability statements are not possible given current scientific understanding.

c. Extreme events

1) STAKEHOLDER PROJECTIONS BASED ON THE DELTA METHOD

Table 7 shows projected changes in the frequency of heat waves, cold events, and coastal flooding in the NYC region. The baseline average number of extreme events per year is shown, along with the central range (middle 67%) of the projections. Because the distribution of extreme events around the (shifting) mean could also change while mean temperature and sea level rise shift, stakeholders were strongly encouraged to focus only on the direction and relative magnitudes of the extreme-event changes in Table 7.

The key finding for most stakeholders is the extent to which mean shifts alone can produce dramatic changes in the frequency of extreme events, such as heat events and coastal storm surges. On the basis of the central range, the number of days per year over 90°F (~32°C) is projected to increase by a factor of approximately 3 by the 2080s. The IPCC-based sea level rise projections alone, without any changes in the historical storm climatological mean and surge levels, lead to a more than threefold increase in the frequency of the baseline 1-in-10-yr coastal flood event by the 2080s.

In contrast to relatively homogeneous mean climate changes, it was emphasized to stakeholders that absolute extreme-event projections like days below freezing and

TABLE 7. Extreme-event projections. For heat and cold events, shown is the central range (middle 67%) of values from model-based distributions, on the basis of 16 GCMs and three emissions scenarios. For coastal floods and storms, shown is the central range (middle 67%) of values from model-based distributions, on the basis of seven GCMs and three emissions scenarios. Decimal places are shown for values of <1 (and for all flood heights). A heat wave is defined as three or more consecutive days with maximum temperature exceeding 90°F (~32°C).

Extreme event	Baseline (1971–2000)	2020s	2050s	2080s
Heat and cold events				
No. of days per year with max temperature >90°F (~32°C)	14	23–29	29–45	37–64
No. of days per year with max temperature >100°F (~38°C)	0.4	0.6–1	1–4	2–9
No. of heat waves per year	2	3–4	4–6	5–8
Avg duration of heat wave (days)	4	4–5	5	5–7
No. of days per year with min temperature ≤32°F (0°C)	72	53–61	45–54	36–49
Coastal floods and storms*				
1-in-10-yr flood to reoccur, on average, ...	~once every 10 yr	~once every 8–10 yr	~once every 3–6 yr	~once every 1–3 yr
Flood heights (m) associated with 1-in-10-yr flood	1.9	2.0–2.1	2.1–2.2	2.3–2.5
1-in-100-yr flood to reoccur, on average, ...	~once every 100 yr	~once every 65–80 yr	~once every 35–55 yr	~once every 15–35 yr
Flood heights (m) associated with 1-in-100-yr flood	2.6	2.7–2.7	2.8–2.9	2.9–3.2

* Does not include the rapid ice melt scenario.

days with more than 1 in. (2.54 cm) of precipitation vary dramatically throughout the metropolitan region, since they depend, for example, on microclimates associated with the urban heat island and proximity to the coast. In a similar way, maps were generated for stakeholders to show that the surge heights for the open estuary at the Battery are higher than corresponding heights in more-protected riverine settings.

It was emphasized to stakeholders that, because of large interannual variability in extremes, even as the climate change signal strengthens, years with relatively few extreme heat events (relative to today's climatological mean) will occur. For example, Central Park's temperatures in 2004 only exceeded 90°F twice. The delta method suggests that not until the middle of this century would such a relatively cool summer (as 2004) feature more days above 90°F than are typically experienced today.

High year-to-year extreme-event variability may already give some stakeholders a framework for assessing sector-specific climate change impacts; even if climate adaptation strategies for extremes are not already in place, short-term benefits may be evident to planners. For example, Central Park in 2010 experienced temperatures of higher than 90°F on 32 different days, which is consistent with projections for a typical year around midcentury. This suggests that some of the infrastructure impacts of extreme heat (such as voltage fluctuations along sagging power lines and increased strain on transportation materials, including rails and asphalt; Horton and Rosenzweig 2010) may have been experienced in 2010 to an extent that may become typical by midcentury. Adaptation strategies designed for an extreme year today (such as a fixed level of mandatory energy use reductions and a fixed level of reductions of train speeds) may be inadequate or unpalatable in the future, however, because of the increase in frequency, duration, and intensity of extreme heat (as an example) associated with climate change (e.g., Meehl et al. 2009; Tebaldi et al. 2006; Meehl and Tebaldi 2004).

2) GCM CHANGES IN INTRA-ANNUAL DISTRIBUTIONS

Because high-frequency events are not simulated well in GCMs, the results described here were not included in the NYC adaptation assessment; they are explored here as an exercise, since there is the possibility of distributional changes in the future. The daily distribution of 1) maximum temperatures¹⁴ in summer (JJA), and 2) minimum temperatures in winter (DJF) are analyzed

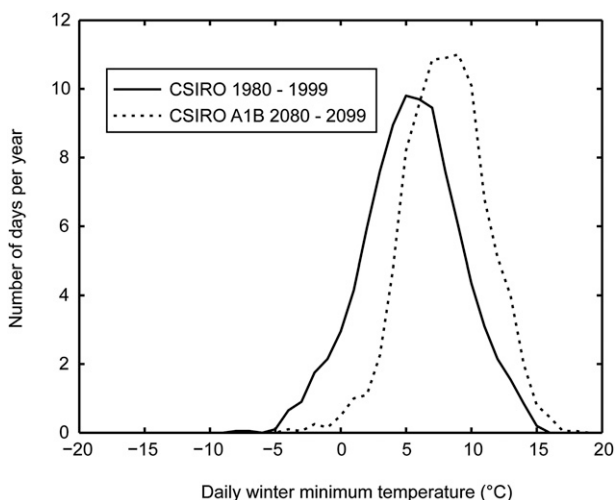


FIG. 8. Daily distribution (number of days per year) of winter (DJF) minimum temperature (°C), for the New York metropolitan region in the CSIRO GCM. Solid line: 1980–99 hindcast; dotted line: 2080–99 A1B scenario.

in the three GCMs described earlier (CSIRO, GISS, and MPI; section 3d), both for the 1980–99 hindcast and the 2080–99 A1B experiment.

The results indicate that GCM temperature changes in the region in some cases do reflect more than a shifting mean. The intra-annual standard deviation¹⁵ of winter minima decreases in all three GCMs (in two cases by approximately 10%), whereas summer standard deviation changes are negligible. One tail of a season's distribution can be more affected than the other; as shown in Fig. 8 for CSIRO, the winter minimum changes are more pronounced on anomalously cold days than on anomalously warm days. All three GCMs show a larger shift in the coldest 1% of the distribution than in the warmest 1%. This asymmetry at the 1% tails is most pronounced in CSIRO, for which the future coldest-1% event occurs 8 times as often in the baseline whereas the baseline warmest-1% event occurs 3 times as often in the future.

d. Comparison of GCM gridbox-based projections with other downscaling methods

The GCM gridbox results used for the New York assessment were compared with statistically downscaled results from bias-corrected and spatially disaggregated (BCSD) climate projections at $1/8^\circ$ resolution derived from the WCRP CMIP3 multimodel dataset. The BCSD projections were obtained online (http://gdo-dcp.ucllnl.org/downscaled_cmip3_projections/; Maurer et al. 2007). Results were also compared with simulations from four

¹⁴ Precipitation was excluded on the basis of the preliminary analysis of hindcast daily precipitation described in section 3d.

¹⁵ As calculated separately for each year and then averaged across the 20 years to minimize the role of interannual variability.

TABLE 8. Pairings of global and regional climate models used from NARCCAP.

GCM driver	RCM	Combination	RCM reference
Geophysical Fluid Dynamics Laboratory	Regional Climate Model, version 3 (RCM3)	RCM3 + GFDL	Pal et al. (2007)
Third-Generation Coupled General Circulation Model (CGCM3)	RCM3	RCM3 + CGCM3	Pal et al. (2007)
CGCM3	Canadian Regional Climate Model (CRCM)	CRCM + CGCM3	Caya and Laprise (1999)
Hadley Centre Coupled Model, version 3 (HadCM3)	Hadley Regional Model 3/Providing Regional Climates for Impacts Studies (HRM3)	HRM3 + HadCM3	Jones et al. (2004)

pairings of GCMs and regional climate models (RCMs; Table 8) contributing to the North American Regional Climate Change Assessment Program (NARCCAP; Mearns et al. 2009). Comparison of the three methods is limited to the 2050s time slice under the A2 emissions scenario relative to the 1970–99 baseline, because NARCCAP projections are not available for other emissions scenarios or time periods. The comparison focuses on projections rather than validation, since the BCSD method by definition includes bias correction whereby the baseline GCM outputs are adjusted to match the observed mean and variance. Preliminary analysis of NARCCAP results indicates that these simulations, like GCM projections, require bias correction.

The ensemble mean changes for the GCM gridbox, BCSD, and RCM approaches differ from each other by no more than 0.3°C for temperature and 3% for precipitation. The intermodel temperature range is slightly larger for the GCM gridbox approach than for BCSD, and the opposite is the case for precipitation. The four RCM simulations perhaps not surprisingly feature a smaller intermodel range than do the 16 ensemble members for the GCM gridbox and BCSD approaches.

The number of days above 90°F was evaluated as a measure of extreme events. The delta method applied to the GCM grid box and BCSD¹⁶ produce virtually identical results (increases of approximately 185% and 180%, respectively, in the number of days above 90°F). When actual daily values from RCMs are used, the increase is approximately 170%. When the delta method from the RCMs is applied to the observations, the increase is approximately 195%.

For mean changes and the daily extreme metric assessed here, BCSD and the four RCMs offer comparable results to the single-gridbox GCM approach in the New York metropolitan region. Future research will assess how statistical and dynamic downscaling perform in more specialized contexts tailored to unique stakeholder

needs that are beyond the scope of the NYC initial assessment. For example, reservoir managers concerned with water turbidity might desire information about sequences of days with intense precipitation during particular times of the year. Future research will also explore the pros and cons of projections that incorporate highly uncertain modeled changes in interannual variance through time.¹⁷

5. Conclusions and recommendations for future work

A framework for climate hazard assessment geared toward adaptation planning and decision support is described. This GCM single-gridbox, delta method–based approach, designed for cities and regions that are smaller than typical GCM gridbox sizes that face resource and time constraints, achieves comparable results in the New York metropolitan region to other statistically and dynamically downscaled products. When applied to high-frequency historical data, long-term mean monthly climate *changes* (which GCMs are expected to simulate more realistically for point locations than they will other features such as *actual* long-term mean climate or high-frequency statistics) yield dramatic changes in the frequency of stakeholder-relevant climate hazards such as coastal flooding and heat events. The precise projections should not be emphasized given the uncertainties, but they are of sufficient magnitude relative to the historical hazard profile to justify development and initial prioritization of adaptation strategies. This process is now well under way in the New York metropolitan region.

When climate-model results for the New York metropolitan region are used only for the calculation of monthly climate change factors based on the differences and ratios between 30-yr future time slices and a 30-yr baseline period, three generalized findings follow. First,

¹⁶ At the time of analysis, BCSD was only available at monthly resolution.

¹⁷ Preliminary analysis reveals that over the New York metropolitan region grid box a slight majority of the GCMs show increasing interannual variance of monthly temperature T and precipitation P whereas a large majority of the BCSD and NARCCAP RCM projections do.

using multiple ensemble members from the same GCM provides little additional information, since the 30-yr average intramodel ranges are smaller than the comparable intermodel range. Second, the spatial pattern of climate change factors in many regions (including New York City) is sufficiently homogeneous—relative to the intermodel range—to justify use of climate change factors from a single overlying GCM grid box. Third, for these metrics, newer statistically (BCSD) and dynamically (four NARCCAP RCMs) downscaled products provide results that are comparable to those of the GCM single-gridbox output used by the NPCC.

The checklist in Table 2 provides a series of questions to help to inform the selection of the most appropriate climate hazard assessment and projection methods. For example, the delta method is more justified when 1) robust, long-term historical statistics are available and 2) evidence of how modes of interannual and interdecadal variability and their local teleconnections will change with climate change is inconclusive. Both of these criteria are met in the NYC metropolitan region. In contrast, more complex applications (than the delta method) of statistically and dynamically downscaled products especially may be more appropriate when spatially continuous projections are needed over larger regions with complex topography. For example, where a large mountain range is associated with a strong precipitation gradient at sub-GCM-gridbox scales, percentage changes in precipitation might also be expected to be more spatially heterogeneous than in the New York metropolitan region.

Extreme-event projections, so frequently sought by stakeholders for impact analysis, will likely improve as statistical and dynamical downscaling evolve. RCMs especially hold promise for assessing how “slow” variations associated with climate change and variability will affect the future distribution of “fast” extremes like sub-daily rainfall events. Nevertheless, translating RCM simulations into stakeholder-relevant projections requires many of the same adjustments and caveats described here for GCMs (such as bias correction). Statistical downscaling techniques also hold promise as well for the simulation of extremes (nonstationarity notwithstanding), to the extent that predictor variables are simulated well by GCMs and are linkable to policy-relevant local climate variables. Projections of extremes will also benefit from improved estimates of historical extremes (such as the 1-in-100-yr drought and coastal flood) as long-term proxy records of tree rings and sediment (as examples) are increasingly utilized.

There is also a need for improved simulation of climate variability at interannual-to-decadal scales, because this is the time horizon for investment decisions

and infrastructure lifetime in many sectors, including telecommunications (Rosenzweig and Solecki 2010). The limits to such predictability are beginning to be explored in Coupled Model Intercomparison Project (CMIP5) experiments initialized with observed ocean data, but this is a long-term research issue.

An absence of local climate projections need not preclude consideration of adaptation. For many locales, climate changes in other regions may rival the importance of local changes by influencing migration, trade, and ecosystem and human health, for example. Furthermore, some hazards such as drought are often regional phenomena, with multistate policy implications (such as water-sharing agreements). Last, since climate vulnerability depends on many nonclimatic factors (such as poverty), some adaptation strategies (such as poverty-reduction measures) can be commenced in advance of climate projections.

Monitoring of climate indicators should be encouraged because it reduces uncertainties and leads to refined projections. On a local scale, sustained high-temporal-resolution observation networks can provide needed microclimatic information, including spatial and temporal variation in extreme events such as convective rainfall and storm-surge propagation. At the global scale, monitoring of polar ice sheets and global sea level will improve understanding of sea level rise. Periodic assessments of evolving climate, impacts and adaptation science will support flexible/recursive adaptation strategies that minimize the impact of climate hazards while maximizing societal benefits.

Acknowledgments. This work was supported by the Rockefeller Foundation. We acknowledge the modeling groups, the Program for Climate Model Diagnosis and Intercomparison (PCMDI) and the WCRP for the CMIP3 multimodel dataset, supported by the Office of Science of the U.S. Department of Energy. We thank Jonathan Gregory for additional GCM output not available from the WCRP dataset. We also thank Adam Freed and Aaron Koch from the Mayor’s Office of Long Term Planning and Sustainability and Malcolm Bowman from the NPCC for comments on prior work that helped to inform this paper. We also thank the anonymous reviewers of this manuscript.

REFERENCES

- Arnell, N. W., 1996: *Global Warming, River Flows, and Water Resources*. John Wiley and Sons, 234 pp.
- ASCE, 2009: *2009 Report Card for America’s Infrastructure*. American Society of Civil Engineers, 153 pp. [Available online at http://www.infrastructurereportcard.org/sites/default/files/RC2009_full_report.pdf.]

- Bardossy, A., and E. Plate, 1992: Space-time model for daily rainfall using atmospheric circulation patterns. *Water Resour. Res.*, **28**, 1247–1259.
- Bindoff, N. L., and Coauthors, 2007: Observations: Oceanic climate change and sea level. *Climate Change 2007: The Physical Science Basis*, S. Solomon et al., Eds., Cambridge University Press, 386–432.
- Bradbury, J. A., B. D. Keim, and C. P. Wake, 2002: U.S. East Coast trough indices at 500 hPa and New England winter climate variability. *J. Climate*, **15**, 3509–3517.
- Brekke, L. D., M. D. Dettinger, E. P. Maurer, and M. Anderson, 2008: Significance of model credibility in estimating climate projection distributions for regional hydroclimatological risk assessments. *Climatic Change*, **89**, 371–394.
- Caya, D., and R. Laprise, 1999: A semi-implicit semi-Lagrangian regional climate model: The Canadian RCM. *Mon. Wea. Rev.*, **127**, 341–362.
- Chen, J. L., C. R. Wilson, D. Blakenship, and B. D. Tapley, 2009: Accelerated Antarctic ice loss from satellite gravity measurements. *Nat. Geosci.*, **2**, 859–862.
- Christensen, J. H., and Coauthors, 2007: Regional climate projections. *Climate Change 2007: The Physical Science Basis*, S. Solomon et al., Eds., Cambridge University Press, 849–940.
- Collins, W. D., and Coauthors, 2006: The Community Climate System Model version 3 (CCSM3). *J. Climate*, **19**, 2122–2143.
- Cubasch, U., and Coauthors, 2001: Projections of future climate change. *Climate Change 2001: The Scientific Basis*, J. T. Houghton et al., Eds., Cambridge University Press, 525–582.
- Delworth, T. L., and Coauthors, 2006: GFDL's CM2 global coupled climate models. Part I: Formulation and simulation characteristics. *J. Climate*, **19**, 643–674.
- Easterling, D. R., T. R. Karl, J. H. Lawrimore, and S. A. Del Greco, 1999: United States Historical Climatology Network daily temperature and precipitation data (1891–1997). Oak Ridge National Laboratory Carbon Dioxide Information Analysis Center Rep. ORNL/CDIAC-118, NDP-070, 84 pp.
- Emori, S., and S. J. Brown, 2005: Dynamic and thermodynamic changes in mean and extreme precipitation under changed climate. *Geophys. Res. Lett.*, **32**, L17706, doi:10.1029/2005GL023272.
- Fairbanks, R. G., 1989: 17,000-year glacio-eustatic sea level record: Influence of glacial melting rates on the Younger Dryas event and deep-ocean circulation. *Nature*, **342**, 637–642.
- Flato, G. M., cited 2010: The Third Generation Coupled Global Climate Model (CGCM3). [Available online at <http://www.ec.gc.ca/ccmac-cccma/default.asp?lang=En&n=1299529F-1>.]
- Furevik, T., M. Bentsen, H. Drange, I. K. T. Kindem, N. G. Kvamstø, and A. Sorteberg, 2003: Description and evaluation of the Bergen climate model: ARPEGE coupled with MICOM. *Climate Dyn.*, **21**, 27–51.
- Gaffin, S. R., and Coauthors, 2008: Variations in New York City's urban heat island strength over time and space. *Theor. Appl. Climatol.*, **94**, 1–11.
- Giorgi, F., and L. O. Mearns, 2002: Calculation of average, uncertainty range, and reliability of regional climate changes from AOGCM simulations via the “reliability ensemble averaging” (REA) method. *J. Climate*, **15**, 1141–1158.
- Gleck, P. H., 1986: Methods for evaluating the regional hydrologic effects of global climate changes. *J. Hydrol.*, **88**, 97–116.
- Gordon, H. B., and Coauthors, 2002: The CSIRO Mk3 Climate System Model. Commonwealth Scientific and Industrial Research Organisation Atmospheric Research Tech. Paper 60, 130 pp.
- Gornitz, V., 2001: Sea-level rise and coasts. *Climate Change and a Global City: The Potential Consequences of Climate Variability and Change—Metro East Coast*, C. Rosenzweig and W. D. Solecki, Eds., Columbia Earth Institute, 121–148.
- Greene, A. M., L. Goddard, and U. Lall, 2006: Probabilistic multimodel regional temperature change projections. *J. Climate*, **19**, 97–116.
- Grinsted, A., J. C. Moore, and S. Jevrejeva, 2009: Reconstructing sea level from paleo and projected temperatures 2000 to 2100 A.D. *Climate Dyn.*, **34**, 461–472.
- Grotch, S. L., and M. C. MacCracken, 1991: The use of general circulation models to predict regional climatic change. *J. Climate*, **4**, 286–303.
- Hansen, J., M. Sato, P. Kharecha, G. Russell, D. W. Lea, and M. Siddall, 2007: Climate changes and trace gases. *Philos. Trans. Roy. Soc.*, **365**, 1925–1954.
- Hayhoe, K., and Coauthors, 2007: Past and future changes in climate and hydrological indicators in the U.S. Northeast. *Climate Dyn.*, **28**, 381–407.
- Hegerl, G. C., and Coauthors, 2007: Understanding and attributing climate change. *Climate Change 2007: The Physical Science Basis*, S. Solomon et al., Eds., Cambridge University Press, 664–745.
- Hill, D., and R. Goldberg, 2001: Energy demand. *Climate Change and a Global City: The Potential Consequences of Climate Variability and Change—Metro East Coast*, C. Rosenzweig and W. D. Solecki, Eds., Columbia Earth Institute, 121–148.
- Hogrefe, C., C. Rosenzweig, P. Kinney, J. Rosenthal, K. Knowlton, B. Lynn, J. Patz, and M. Bell, 2004: Health impacts from climate-change induced changes in ozone level in 85 United States cities. *Epidemiology*, **15**, 94–95.
- Horton, R., and C. Rosenzweig, 2010: Climate risk information. *Climate Change Adaptation in New York City: Building a Risk Management Response*, C. Rosenzweig, and W. Solecki, Eds., New York Academy of Sciences, 148–228.
- , C. Herweijer, C. Rosenzweig, J. P. Liu, V. Gornitz, and A. C. Ruane, 2008: Sea level rise projections for current generation CGCMs based on the semi-empirical method. *Geophys. Res. Lett.*, **35**, L02715, doi:10.101029/02007GL032486.
- Hu, A., G. A. Meehl, W. Han, and J. Yin, 2009: Transient response of the MOC and climate to potential melting of the Greenland Ice Sheet in the 21st century. *Geophys. Res. Lett.*, **36**, L10707, doi:10.1029/2009GL037998.
- Johns, T. C., and Coauthors, 2006: The new Hadley Centre climate model HadGEM1: Evaluation of coupled simulations. *J. Climate*, **19**, 1327–1353.
- Jones, R. G., and Coauthors, 2004: Generating high-resolution climate change scenarios using PRECIS. MET Office Hadley Centre.
- Jungclaus, J. H., and Coauthors, 2006: Ocean circulation and tropical variability in the coupled model ECHAM5/MPI-OM. *J. Climate*, **19**, 3952–3972.
- K-1 Model Developers, 2004: K-1 Technical Report. Center for Climate System Research, University of Tokyo, 34 pp.
- Kanamitsu, M., W. Ebisuzaki, J. Woollen, S.-K. Yang, J. J. Hnilo, M. Fiorino, and G. L. Potter, 2002: NCEP–DOE AMIP-II Reanalysis (R-2). *Bull. Amer. Meteor. Soc.*, **83**, 1631–1643.
- Karl, T. R., C. N. Williams, F. T. Quinlan, and T. A. Boden, 1990: United States Historical Climatology Network (HCN) serial temperature and precipitation data. Oak Ridge National Laboratory Carbon Dioxide Information and Analysis Center Environmental Science Division Publ. 304, 389 pp.
- Kinney, P. L., D. Shindell, E. Chae, and B. Winston, 2001: Public health. *Climate Change and a Global City: The Potential*

- Consequences of Climate Variability and Change—Metro East Coast*, C. Rosenzweig and W. D. Solecki, Eds., Columbia Earth Institute, 103–120.
- Le Quere, C., and Coauthors, 2009: Trends in the sources and sinks of carbon dioxide. *Nat. Geosci.*, **2**, 831–836.
- Marti, O., and Coauthors, 2005: The New IPSL Climate System Model: IPSL-CM4. Institut Pierre Simon Laplace des Sciences de l'Environnement Global Note du Pôle de Modélisation 26, 84 pp.
- Maurer, E. P., L. Brekke, T. Pruiitt, and P. B. Duffy, 2007: Fine-resolution climate projections enhance regional climate change impact studies. *Eos, Trans. Amer. Geophys. Union*, **88**, 504.
- Mearns, L. O., W. Gutowski, R. Jones, R. Leung, S. McGinnis, A. Nunes, and Y. Qian, 2009: A regional climate change assessment program for North America. *Eos, Trans. Amer. Geophys. Union*, **90**, 311.
- Meehl, G. A., and C. Tebaldi, 2004: More intense, more frequent, and longer lasting heat waves in the 21st century. *Science*, **305**, 994–997.
- , J. M. Arblaster, and C. Tebaldi, 2005: Understanding future patterns of increased precipitation intensity in climate model simulations. *Geophys. Res. Lett.*, **32**, L18719, doi:10.1029/2005GL023680.
- , C. Covey, K. E. Taylor, T. Delworth, R. J. Stouffer, M. Latif, B. McAvaney, and J. F. B. Mitchell, 2007a: The WCRP CMIP3 multimodel dataset: A new era in climate change research. *Bull. Amer. Meteor. Soc.*, **88**, 1383–1394.
- , and Coauthors, 2007b: Global climate projections. *Climate Change 2007: The Physical Science Basis*, S. Solomon et al., Eds., Cambridge University Press, 747–845.
- , C. Tebaldi, G. Walton, D. Easterling, and L. McDaniel, 2009: Relative increase of record high maximum temperatures compared to record low minimum temperatures in the U.S. *Geophys. Res. Lett.*, **36**, L23701, doi:10.1029/2009GL040736.
- Min, S.-K., S. Legutke, A. Hense, and W.-T. Kwon, 2005: Climatology and internal variability in a 1000-year control simulation with the coupled climate model ECHO-G—I. Near-surface temperature, precipitation and mean sea level pressure. *Tellus*, **57A**, 605–621.
- Mitrovica, J. X., M. Tamisiea, J. L. Davis, and G. A. Milne, 2001: Recent mass balance of polar ice sheets inferred from patterns of global sea-level change. *Nature*, **409**, 1026–1029.
- , N. Gomez, and P. U. Clark, 2009: The sea-level fingerprint of West Antarctic collapse. *Science*, **323**, 753.
- Mote, P., A. Petersen, S. Reeder, H. Shipman, and W. Binder, 2008: Sea level rise in the coastal waters of Washington State. University of Washington Climate Impacts Group and the Washington Department of Ecology Rep., 11 pp.
- MTA, 2007: August 8, 2007 storm report. Metropolitan Transportation Authority Rep., 115 pp. [Available online at http://www.mta.info/mta/pdf/storm_report_2007.pdf.]
- Nakicenovic, N., and Coauthors, 2000: *Special Report on Emissions Scenarios*. Cambridge University Press, 599 pp.
- Namias, J., 1966: Nature and possible causes of the northeastern United States drought during 1962–65. *Mon. Wea. Rev.*, **94**, 543–554.
- National Research Council, 2009: *Informing Decisions in a Changing Climate*. The National Academies Press, 200 pp.
- , 2010a: *Advancing the Science of Climate Change*. America's Climate Choices Series, The National Academies Press, 528 pp.
- , 2010b: *Adapting to the Impacts of Climate Change*. America's Climate Choices Series, The National Academies Press, 292 pp.
- New York City Office of the Mayor, 2009: Mayor Bloomberg releases New York City Panel on Climate Change report that predicts higher temperatures and rising sea levels for New York City. NYC press release. [Available online at www.nyc.gov/html/om/html/2009a/pr079-09.html.]
- Nicholls, R. J., S. Hanson, and C. Herweiger, 2008: Ranking port cities with high exposure and vulnerability to climate extremes: Exposure estimates. OECD Environment Working Paper 1, 63 pp.
- NYCDEP, 2008: Assessment and action plan: A report based on the ongoing work of the DEP Climate Change Task Force. NYCDEP Climate Change Program Rep. 1, 102 pp. [Available online at http://www.nyc.gov/html/dep/pdf/climate/climate_complete.pdf.]
- Pal, J. S., and Coauthors, 2007: Regional climate modeling for the developing world: The ICTP RegCM3 and RegCM3. *Bull. Amer. Meteor. Soc.*, **88**, 1395–1409.
- Peltier, W. R., 2001: Global glacial isostatic adjustment and modern instrumental records of relative sea level history. *Sea Level Rise: History and Consequences*, B. C. Douglas, M. S. Kearney, and S. P. Leatherman, Eds., Academic Press, 65–95.
- , and R. G. Fairbanks, 2006: Global glacial ice volume and last glacial maximum duration from an extended Barbados sea level record. *Quat. Sci. Rev.*, **25**, 3322–3337.
- Pfeffer, W. T., J. T. Harper, and S. O'Neel, 2008: Kinematic constraints on glacier contributions to 21st-century sea-level rise. *Science*, **321**, 1340–1343.
- PlaNYC, 2008: Sustainable stormwater management plan 2008. Mayor's Office of Long-Term Planning and Sustainability Rep., 112 pp. [Available online at http://nytelecom.vo.llnwd.net/o15/agencies/planyc2030/pdf/nyc_sustainable_stormwater_management_plan_final.pdf.]
- Rahmstorf, S., 2007: A semi-empirical approach to projections future sea level rise. *Science*, **315**, 368–370.
- Randall, D. A., and Coauthors, 2007: Climate models and their evaluation. *Climate Change 2007: The Physical Science Basis*, S. Solomon et al., Eds., Cambridge University Press, 590–662.
- Rignot, E., and A. Cazenave, 2009: Ice sheets and sea level rise feedbacks. *Arctic Climate Feedbacks: Global Implications*, M. Sommerkorn and S. J. Hassol, Eds., WWF International Arctic Programme, 39–53.
- Rind, D., M. Chin, G. Feingold, D. Streets, R. A. Kahn, S. E. Schwartz, and H. Yu, 2009: Modeling the effects of aerosols on climate. Aerosol properties and their impacts on climate, U.S. Climate Change Science Program Synthesis and Assessment Product 2.3, M. Chin, R. A. Kahn, and S. E. Schwartz, Eds., National Aeronautics and Space Administration, 64–97.
- Rohling, E. J., K. Grant, C. H. Hemleben, M. Siddall, B. A. A. Hoogakker, M. Bolshaw, and M. Kucery, 2008: High rates of sea-level rise during the last interglacial period. *Nat. Geosci.*, **1**, 38–42.
- Rosenzweig, C., and W. D. Solecki, Eds., 2001: *Climate Change and a Global City: The Potential Consequences of Climate Variability and Change—Metro East Coast*. Columbia Earth Institute, 224 pp.
- , and —, Eds., 2010: Climate change adaptation in New York City: Building a risk management response. New York City Panel on Climate Change 2010 Rep., Annals of the New York Academy of Sciences, Vol. 1196, 354 pp.
- , —, L. Parshall, and S. Hodges, Eds., 2006: Mitigating New York City's heat island with urban forestry, living roofs, and light surfaces. New York State Energy Research and

- Development Authority New York City Regional Heat Island Initiative Final Rep. 06-06, 133 pp.
- , D. C. Major, K. Demong, C. Stanton, R. Horton, and M. Stults, 2007: Managing climate change risks in New York City's water system: Assessment and adaptation planning. *Mitigation Adapt. Strategies Global Change*, **12**, 1391–1409.
- Schmidt, G. A., and Coauthors, 2006: Present-day atmospheric simulations using GISS ModelE: Comparison to in situ, satellite and reanalysis data. *J. Climate*, **19**, 153–192.
- Shepherd, A., and D. Wingham, 2007: Recent sea-level contributions of the Antarctic and Greenland Ice Sheets. *Science*, **315**, 1529–1532.
- Smith, R. L., C. Tebaldi, D. Nychka, and L. O. Mearns, 2009: Bayesian modeling of uncertainty in ensembles of climate models. *J. Amer. Stat. Assoc.*, **104**, 97–116.
- Solecki, W. D., L. Patrick, and M. Brady, 2010: Climate protection levels: Incorporating climate change into design and performance standards. Climate change adaptation in New York City: Building a risk management response. New York City Panel on Climate Change 2010 Rep., Annals of the New York Academy of Sciences, C. Rosenzweig and W. D. Solecki, Eds., Vol. 1196, New York Academy of Sciences, 294–351.
- Solomon, S., D. Qin, M. Manning, M. Marquis, K. Averyt, M. M. B. Tignor, H. L. Miller Jr., and Z. Chen, Eds., 2007: *Climate Change 2007: The Physical Science Basis*. Cambridge University Press, 996 pp.
- Sussman, E., and D. C. Major, 2010: Law and regulation. Climate change adaptation in New York City: Building a risk management response. New York City Panel on Climate Change 2010 Rep., Annals of the New York Academy of Sciences, C. Rosenzweig and W. D. Solecki, Eds., Vol. 1196, New York Academy of Sciences, 87–112.
- Tebaldi, C., R. L. Smith, D. Nychka, and L. O. Mearns, 2005: Quantifying uncertainty in projections of regional climate change: A Bayesian approach to the analysis of multimodel ensembles. *J. Climate*, **18**, 1524.
- , K. Hayhoe, J. M. Arblaster, and G. A. Meehl, 2006: Going to the extremes: An intercomparison of model-simulated historical and future changes in extreme events. *Climatic Change*, **79**, 185–211.
- Terray, L. S., S. Valcke, and A. Piacentini, 1998: OASIS 2.2 guide and reference manual. Centre Europeen de Recherche et de Formation Avancée en Calcul Scientifique Tech. Rep. TR/CMGC/98-05.
- Volodin, E. M., and N. A. Diansky, 2004: El-Niño reproduction in a coupled general circulation model of atmosphere and ocean. *Russ. Meteor. Hydrol.*, **12**, 5–14.
- Washington, W. M., and Coauthors, 2000: Parallel climate model (PCM) control and transient simulations. *Climate Dyn.*, **16**, 755–774.
- Weiss, J., J. Overpeck, and B. Strauss, 2011: Implications of recent sea level rise science for low-elevation areas in coastal cities of the conterminous U.S.A. *Climatic Change*, **105**, 635–645, doi:10.1007/s10584-011-0024-x.
- Wigley, T. M., P. D. Jones, K. Briffa, and G. Smith, 1990: Obtaining sub-grid-scale information from coarse-resolution general circulation model output. *J. Geophys. Res.*, **95**, 1943–1953.
- Wilby, R. L., T. M. L. Wigley, D. J. Conway, P. D. Jones, B. C. Hewitson, J. Main, and D. S. Wilks, 1998: Statistical downscaling of general circulation model output: A comparison of methods. *Water Resour. Res.*, **34**, 2995–3008.
- , C. W. Dawson, and E. M. Barrow, 2002: SDSM—A decision support tool for the assessment of regional climate change impacts. *Environ. Model. Software*, **17**, 145–157.
- , S. Charles, E. Zorita, B. Timbal, P. Whetton, and L. Mearns, 2004: Guidelines for use of climate scenarios developed from statistical downscaling methods. IPCC Supporting Material, 27 pp. [Available online at <http://www.narccap.ucar.edu/doc/tgica-guidance-2004.pdf>.]
- Williams, C. N., M. J. Menne, R. S. Vose, and D. R. Easterling, 2005: United States Historical Climatology Network monthly temperature and precipitation data. Oak Ridge National Laboratory Carbon Dioxide Information Analysis Center Rep. ORNL/CDIAC-118, NDP-019.
- Wood, A. W., L. R. Leung, V. Sridhar, and D. P. Lettenmaier, 2004: Hydrologic implications of dynamical and statistical approaches to downscaling climate model outputs. *Climatic Change*, **62**, 189–216.
- World Meteorological Organization, 1989: Calculation of monthly and annual 30-year standard normals. WCDP 10 and WMO-TD 341, World Meteorological Organization.
- Yin, J., M. E. Schlesinger, and R. J. Stouffer, 2009: Model projections of rapid sea-level rise on the northeast coast of the United States. *Nat. Geosci.*, **15**, 1–5.
- Yukimoto, S., and A. Noda, 2003: Improvements of the Meteorological Research Institute Global Ocean-Atmosphere Coupled GCM (MRI-GCM2) and its climate sensitivity. National Institute for Environmental Studies CGER Supercomputing Activity Rep.